Magnetic field amplification during core collapse

Martin Obergaulinger

CAMAP, Departament d´Astronomia i Astrofísica, Universitat de València

Physics of Neutron Stars, St Petersburg, 11 July 2017

Collaborators

- At MPA, Garching: Ewald Müller, Thomas Janka, Jerome Guilet
- At RIKEN, Tokyo: Oliver Just
- In the CAMAP group in València: Miguel Ángel Aloy, Pablo Cerdá Durán, Tomasz Rembiasz

Motivations for considering magnetic fields

- Note: even if no field is detected in SN ejecta, the central engine may be magnetised. The field can dissipate after the onset of the explosion.
- bipolar geometry of some explosions
- pulsar kicks
- hyper-energetic SNe and GRBs
- magnetic fields of neutron stars

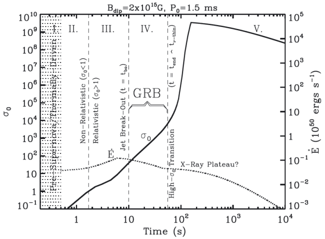

Figure 2. Wind power $\dot{E}$ (right-hand axis) and magnetization σ_0 (left-hand axis; equation 2) of the protomagnetar wind as a function of time since core bounce, calculated for a NS with mass $M_{ns} = 1.4\,M_\odot$, initial spin period $P_0 = 1.5$ ms, surface dipole field strength $B_{dip} = 2 \times 10^{15}$ G and magnetic obliquity $\chi = \pi/2$. Stages denoted I–V are described in detail in Section 3.

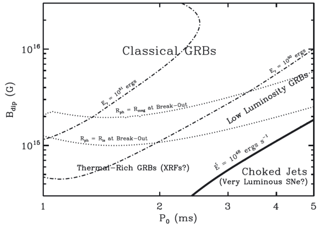

Figure 19. Regimes of high-energy phenomena produced by magnetar birth in core-collapse SNe, as a function of the magnetic dipole field strength, B_{dip}, and initial rotation period, P_0, calculated for an aligned rotator ($\chi = 0$).

Metzger et al. (2011)

Motivations for considering magnetic fields

- Note: even if no field is detected in SN ejecta, the central engine may be magnetised. The field can dissipate after the onset of the explosion.
- bipolar geometry of some explosions
- pulsar kicks
- hyper-energetic SNe and GRBs
- magnetic fields of neutron stars

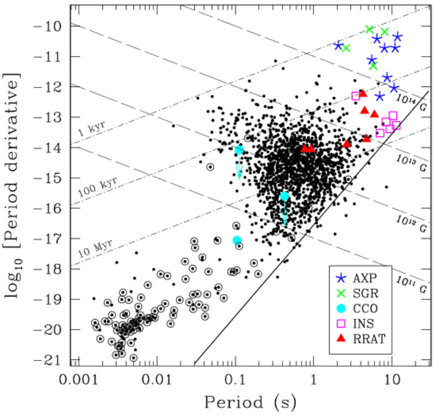

P-$\dot{P}$ diagram of neutron stars (taken from Kaspi, 2010)

Evolution of the magnetic field

Induction equation

- $\partial_t \vec{b} = -c \vec{\nabla} \times \vec{E}$
- $\vec{E} = -\frac{\vec{v}}{c} \times \vec{b} \; (+\frac{c}{4\pi\sigma} \vec{\nabla} \times \vec{b})$
- flux conservation, $\vec{\Phi} = \int_{\mathrm{dA}} \vec{b}$
- divergence constraint: $\vec{\nabla} \cdot \vec{b} = 0$
- ideal MHD: helicity conservation

Lorentz force

- pressure, $P_{\mathrm{mag}} = e_{\mathrm{mag}} = \frac{1}{2} \vec{b}^2$; resists compression
- magnetic tension; resists bending

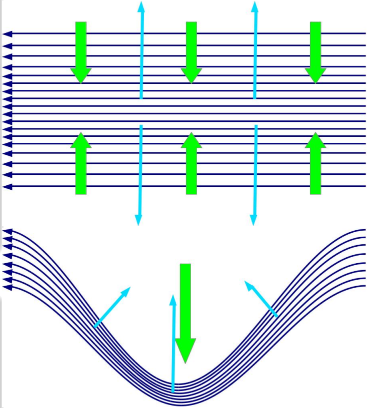

What do magnetic fields add to the SN that other effects don't already imply?

- turbulence, small-scale flows $\rightarrow$ effective viscosity
- contribution to pressure
- large-scale (angular-)momentum, energy transport
- inverse cascade, dynamo
- MRI: instability of differential rotation

Requirements and difficulties

- the usual wishlist for SNe: hydro, nuclear EOS, relativistic gravity, neutrinos
- MHD suffers a lot from dimensional restrictions $\rightarrow$ 3D!
- small-scale phenomena can be quite important $\rightarrow$ high resolution
- evolution depends on field strength and topology $\rightarrow$ large parameter space, dependence on (unknown) pre-collapse state (3d stellar evolution would be nice)
- alternative approach: local simulations

What I'm not considering

- Effects of the magnetic field on the nuclear EOS. Interesting effects may occur (up to a deformation of the PNS), but only if $\vec{b}$ is close to equipartition with the internal energy, which requires super-magnetar fields.
- Possible modifications of the interaction of matter with neutrinos. Uncertain, and ν transport is complex enough as it is.
- Crust, superconductivity and superfluidity. Important on longer time scales as the PNS cools.

- conservation of magnetic flux through a surface

$\rightarrow$ $B \propto \rho^{2/3}$ for a fluid element; energy grows faster than gravitational

- no change of field topology
- core collapse: factor of 10^3 in field strength
- possible saturation: $e_{\mathrm{mag}} \sim e_{\mathrm{kin,r}}$ is unrealistic in collapse
- occurs in every collapse (and continues after bounce)

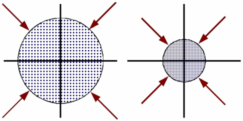

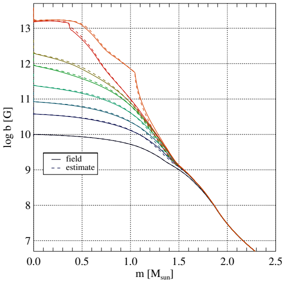

Profiles of field strength during collapse compared to estimate based on flux conservation (deviations come from non-radial geometry)

Structure of the field

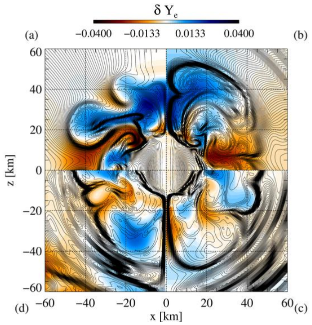

Snapshots of the PNS convection zone at four times after bounce: deviation of Y_e from the angular average and field lines.

- innermost 10 km: stable, no convection → simple structure
- convection layer: multiple overturns, field is concentrated between the convective rolls; highly variables
- surrounding stable layer: magnetic flux accreted from the exterior piles up in a layer of lateral field
- PNS is "shielded" by thick magnetic field
- consequences: may suppress cross-field flows, slow reconnection

Convection/SASI

- hydro instabilities develop quickly
- highly variable amplitude of the instability, flow field
- field is amplified in thin filaments
- final field strength depends on the initial field, and amplification is not (necessarily) leading to equipartition

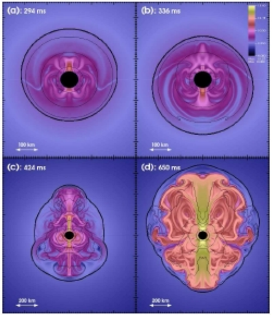

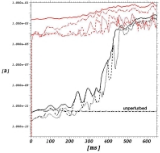

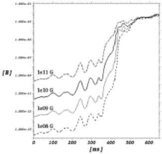

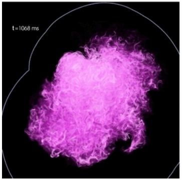

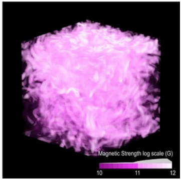

Endeve et al. (2010,2012)

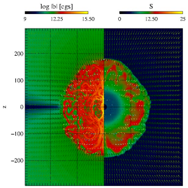

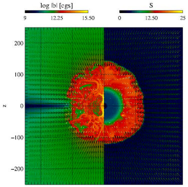

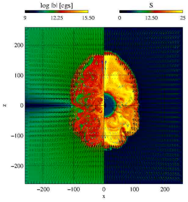

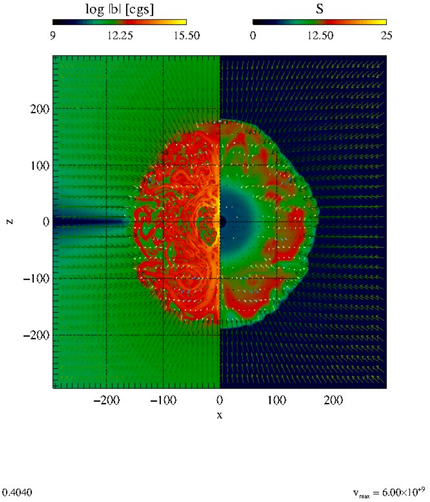

Obergaulinger et al. (2014)

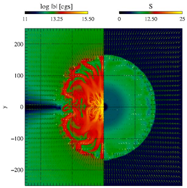

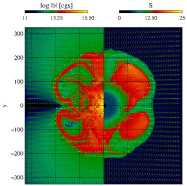

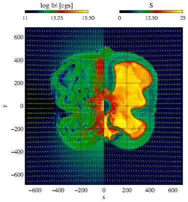

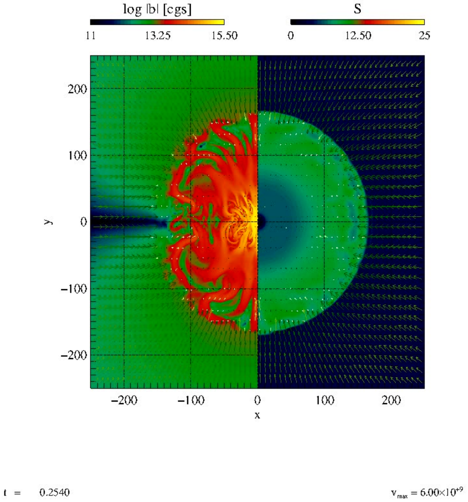

Obergaulinger et al. (2014)

Amplification of Alfvén waves

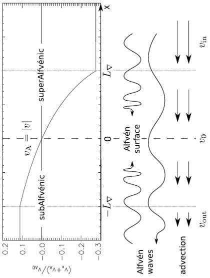

Guilet et al. (2011)

- requires an accretion flow decelerated above the PNS and a (radial) guide field

→ accretion is sub-/super-Alfvén ic inside/outside the Alfvén surface

- Alfvén waves propagating along the field are amplified at the Alfvén point
- waves are finally dissipated there → additional heating
- in core collapse: efficient for a limited parameter range (strong guide field); strong time variability of the Alfvén surface may be a problem
- modelling issues: high resolution, uncertainties in the dissipation

Amplification of Alfvén waves

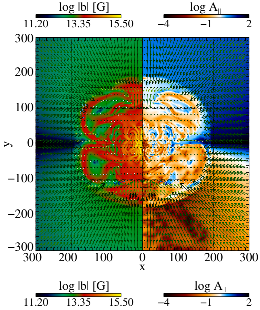

- requires an accretion flow decelerated above the PNS and a (radial) guide field

→ accretion is sub-/super-Alfvén ic inside/outside the Alfvén surface

- Alfvén waves propagating along the field are amplified at the Alfvén point
- waves are finally dissipated there → additional heating
- in core collapse: efficient for a limited parameter range (strong guide field); strong time variability of the Alfvén surface may be a problem
- modelling issues: high resolution, uncertainties in the dissipation

Rotation and magnetic field

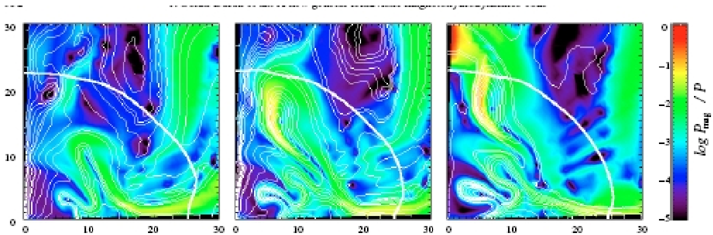

Cerdá-Durán et al. (2008): MRI channel modes

- winding of field lines
- *strong field*: MRI observable
- angular-momentum transport
- jet formation
- MHD explosions visible in the GW signal

Rotation and magnetic field

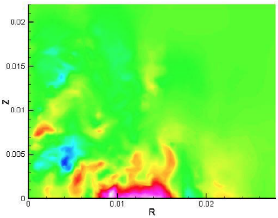

Fig. 3. Toroidal magnetic field distribution at the moment of its maximal energy.

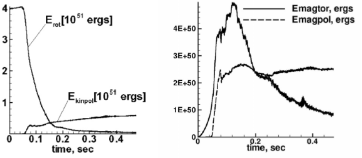

Fig. 4. Time dependence of rotational, kinetic poloidal, and magnetic energies during explosion for a quadrupole-like field, from 5).

Bisnovatyi-Kogan & Moiseenko, (2008)

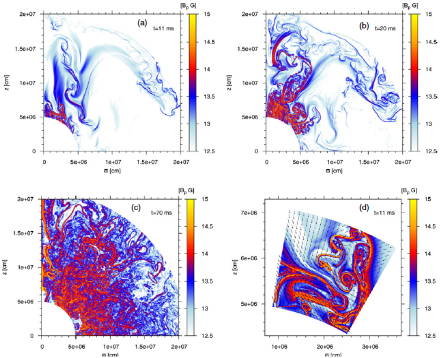

Sawai et al. (2013)

Rotation and magnetic field

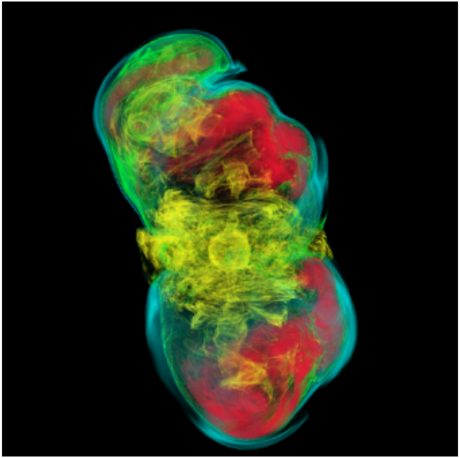

Mösta et al. (2014)

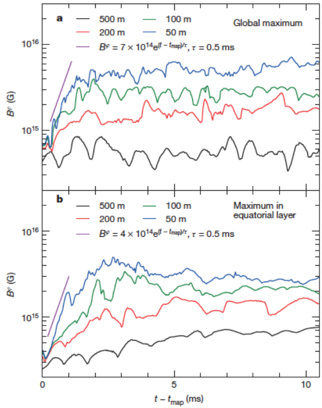

Figure 1 | Evolution of the maximum toroidal magnetic field. Both panels show the maximum toroidal magnetic field (B^{φ}) as a function of time for the four resolutions 500 m, 200 m, 100 m and 50 m. **a**, The global maximum field; **b**, the maximum field in a thin layer above and below the equatorial plane ($-7.5\,\text{km} \leq z \leq 7.5\,\text{km}$). The magenta line indicates exponential growth with an exponential-folding time of $\tau = 0.5$ ms.

Mösta et al. (2015)

Amplification of MHD waves

- given the velocity of MHD waves and a time scale

→ we need to resolve the propagation distance of the waves with n grid cells

- even if the time scale of the wave motion is large (set by large-scale physics), this can prove prohibitive for slow waves

Amplification of MHD waves

- given the velocity of MHD waves and a time scale

→ we need to resolve the propagation distance of the waves with n grid cells

- even if the time scale of the wave motion is large (set by large-scale physics), this can prove prohibitive for slow waves
- example: the MRI is the weak-field instability of the slow mode, with $c_{\text{slow}} \ll c_{\text{s}}, v$
- the length scale can be estimated from the Alfvén velocity and the rotational period

→ $\lambda_{\text{MRI}} = \mathcal{O}(c_{\text{A}}\Omega^{-1})$

Amplification of MHD waves

MRI dispersion

normalised growth rate

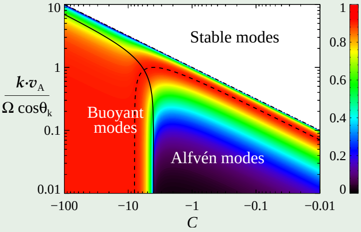

dashed line: fastest growing mode
solid line: boundary between modes branches

Stable modes short modes are stablised by magnetic tension

Alfvén modes fast growth only for finite wave number; CCSNe: $\lambda_{\mathrm{MRI}} \sim$ cm...m

Bouyant modes appear only for large entropy gradient; fast growth for long modes

Definition of symbols

$$\mathcal{C} = \frac{(N)^2 + \left(\varpi \times \partial_\varpi \Omega^2\right)^2}{\Omega^2}$$

N = bouyancy frequency

$\mathbf{v}_A$ = Alfven velocity

$\mathbf{k}$ = wave number

θ_k = angle between $\mathbf{k}$ and the vertical

MRI and neutrinos

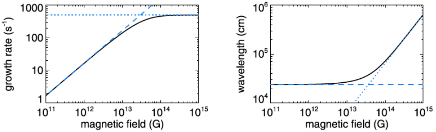

Figure 4. Growth rate (left) and wavelength (right) of the fastest growing MRI mode in the viscous regime as a function of the magnetic field strength for the following fiducial parameters: $\nu = 2 \times 10^{10}\,\mathrm{cm^2\,s^{-1}}$, $\rho = 10^{13}\,\mathrm{g\,cm^{-3}}$ and $\Omega = 1000\,\mathrm{s^{-1}}$. The solid black line shows the numerical solution of the dispersion relation (equation 11). The dashed line shows the asymptotic behaviour in the viscous regime ($E_\nu \ll 1$), given by equations (15) and (16). The dotted line shows the asymptotic behaviour in the ideal regime ($E_\nu \gg 1$), given by equations (4) and (5).

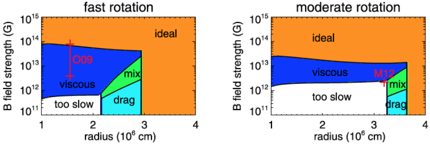

Figure 10. Different regimes of MRI growth as a function of radius and magnetic field strength in the case of fast rotation (left-hand panel) and moderate rotation (right-hand panel), for a PNS model at $t = 170$ ms post-bounce. See the text for a description of the different regimes. The parameter range used in the simulations by Obergaulinger et al. (2009) is shown in red on the left-hand panel, and the parameters assumed by Masada et al. (2012) are shown with a red cross on the right-hand panel. The black lines separating the different regimes are defined as follows. The vertical line separating the 'too slow' and drag MRI regimes corresponds to equation (39). The vertical line between the drag and ideal MRI regimes corresponds to $\Gamma = \Omega$ (which also represents within a numerical factor the condition that the viscous MRI wavelength is longer than the neutrino mean free path). The line separating the 'too slow' and viscous regimes corresponds to equation (19). The almost horizontal line separating the viscous and ideal MRI regimes is given by equation (13). The line separating the drag and mixed regimes shows where the MRI wavelength in the drag regime equals the electron neutrino mean free path (equation 40). Finally, the line separating the mixed and viscous regimes is defined by the equality of the growth rates in the viscous and the drag regimes (equation 41). The last criterion is only approximate, based on the assumption that the growth rate in the mixed regime lies in between those predicted by the drag and viscous formalisms.

Guilet et al. (2015)

- inside the PNS, neutrinos are closely coupled to matter

→ effective neutrino viscosity or drag

- notable deviations from ideal MHD
- suppression of the MRI for relatively weak seed field (MRI wavelength < neutrino mean free path)

MRI termination

- equipartition, $e_{\mathrm{mag}} \sim e_{\mathrm{diffrot}}$, overestimates the final state
- MRI is quenched earlier by secondary instabilities
- linear evolution: channel modes
- Kelvin-Helmholtz or tearing modes disrupt the MRI channel flows

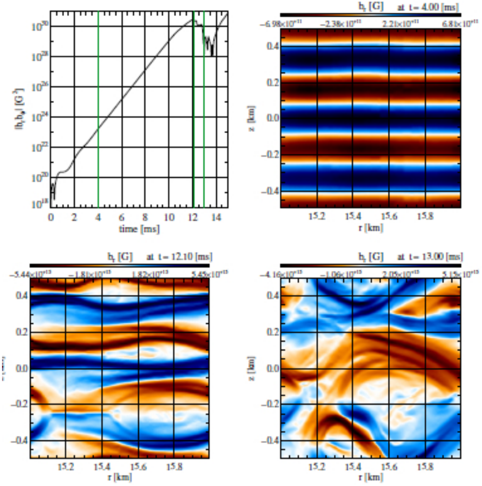

Tomasz Rembiasz (2013): 2d MRI shearing box with viscosity and resistivity.

MRI termination

Pessah (2010)

- perturbations $(\delta b, \delta v)$ of an MRI mode grow at constant rate σ_{MRI}
- MRI channel modes are separated by current sheets and shear layers $\rightarrow$ unstable against parasitic instabilities: Kelvin-Helmholtz and tearing modes

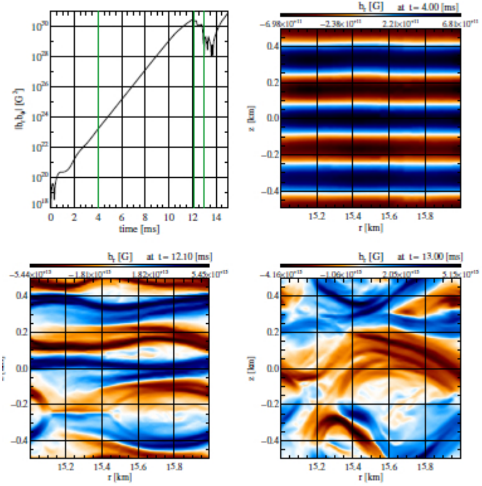

Tomasz Rembiasz (2013): 2d MRI shearing box with viscosity and resistivity.

MRI termination

Pessah (2010)

- parasites grow at rates $\propto B_{\mathrm{MRI}}/\lambda \propto \exp \sigma_{\mathrm{MRI}} t / B_0$, i.e., faster as the MRI proceeds
- at some point, they overtake the MRI and break the channels down into turbulence

$\rightarrow$ MRI growth stops, termination field is set

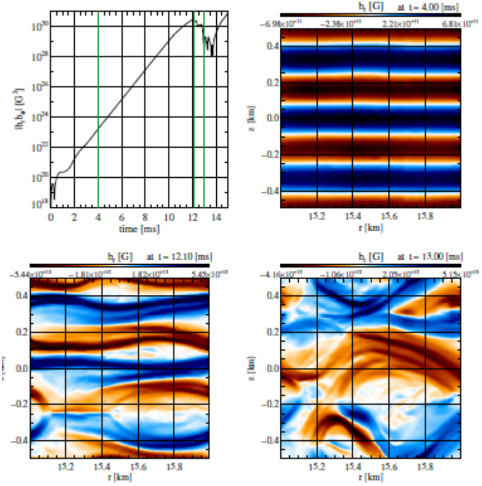

Tomasz Rembiasz (2013): 2d MRI shearing box with viscosity and resistivity.

MRI termination

- can we test this model?
- in principle yes, but...
- identification of instabilities is complex
- you have to carefully distinguish physics from numerics
- numerical errors introduce an effective viscosity/resistivity and modify the growth of the parasitic instabilities

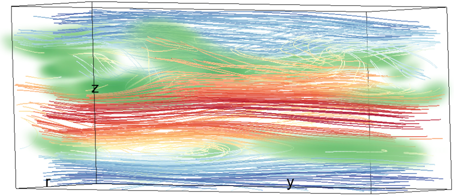

Field lines and current density in a 3d box

What can we say about the parasites?

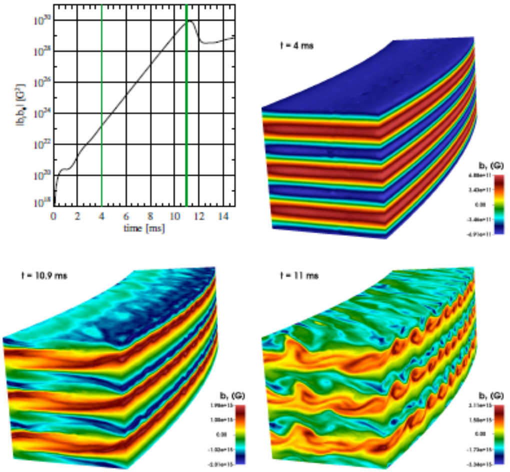

A 3d MRI box: initial phase of perfect channel modes; onset and growth of parasitic instabilities; disruption of channels; turbulence.
Rembiasz et al. (2015)

What can we say about the parasites?

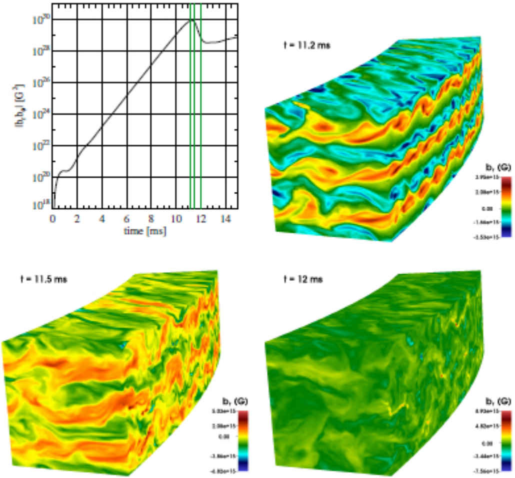

A 3d MRI box: initial phase of perfect channel modes; onset and growth of parasitic instabilities; disruption of channels; turbulence.
Rembiasz et al. (2015)

What can we say about the parasites?

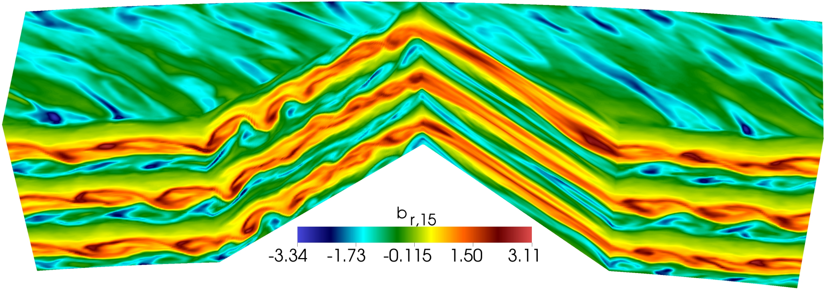

Slicing the box along the axes of the velocity and the magnetic field (indeed 45° as predicted by Pessah). KH instability should be visible in the former plane.

What can we say about the parasites?

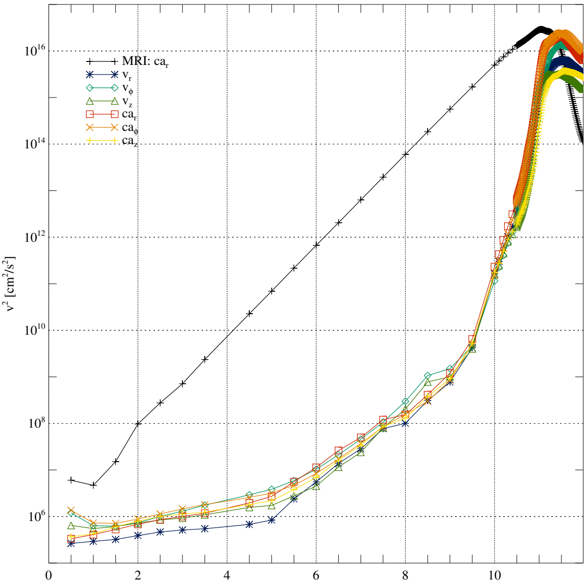

Fourier analysis of the magnetic field in the box. We can distinguish between contributions of the MRI and of the parasites. Parasites grow very rapidly towards termination.

Axisymmetric magnetorotational core collapse

Obergaulinger & Aloy (2017)

35OC

- Woosley & Heger (2006)
- $M_{\rm ZAMS} = 35\,M_\odot$
- includes rotation and magnetic fields according to the Spruit (2002) dynamo
- low mass loss $\rightarrow \sim 28\,M_\odot$ at collapse, rapid rotation
- compactness (O'Connor & Ott, 2011) $\xi_{2.5} = 0.46$
- run with its original magnetic field and with weak and strong artificial fields

z35.0

- Woosley et al. (2002)
- $M_{\rm ZAMS} = 35\,M_\odot$
- zero metallicity
- $\xi_{2.5} = 0.56$
- neither rotation nor magnetic fields in the stellar evolution model
- artificial moderate and rapid rotation and magnetic fields

Obergaulinger & Aloy (2017)

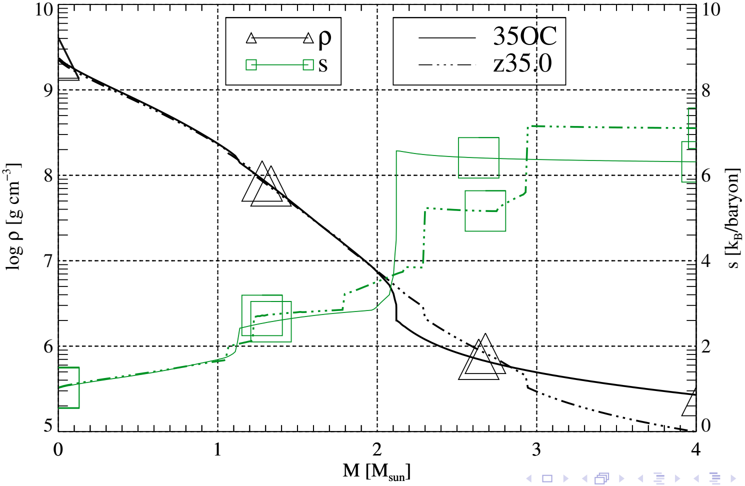

(a)

Evolutionary paths

- 35OC, moderate rotation, weak field: explodes mostly by neutrinos and hydro

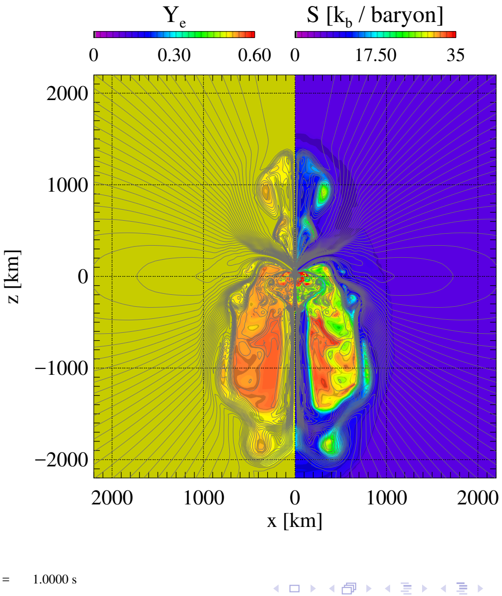

Evolutionary paths

- 35OC, moderate rotation, weak field: explodes mostly by neutrinos and hydro
- 35OC, fast, weak: jet-like explosion

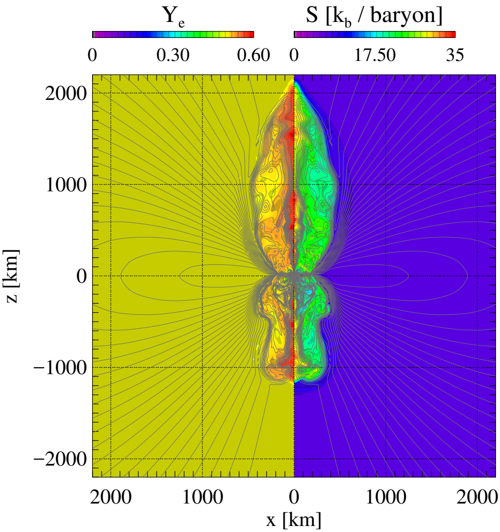

t = 0.8000 s

- 35OC, moderate rotation, weak field: explodes mostly by neutrinos and hydro
- 35OC, fast, weak: jet-like explosion
- 35OC, fast, strong: magneto-rotational jets

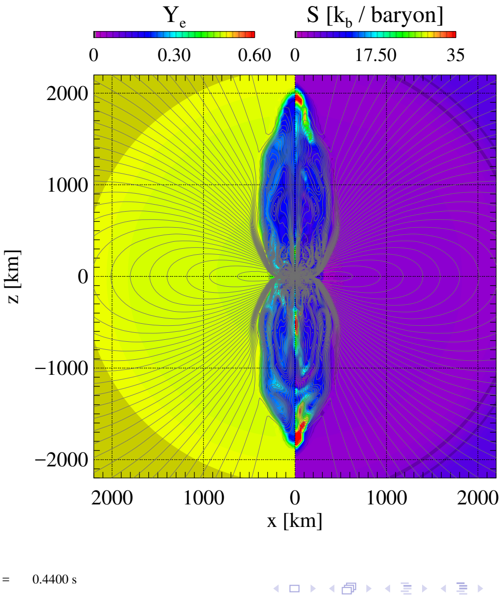

Evolutionary paths

- 35OC, moderate rotation, weak field: explodes mostly by neutrinos and hydro
- 35OC, fast, weak: jet-like explosion
- 35OC, fast, strong: magneto-rotational jets
- z35, slow, weak: no explosion for a very long time

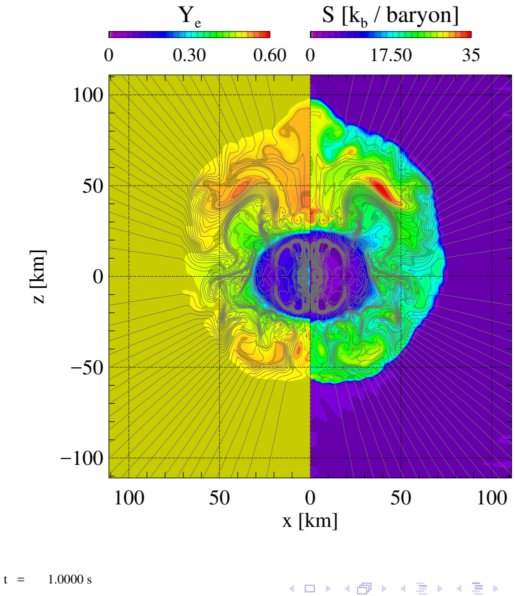

- 35OC, moderate rotation, weak field: explodes mostly by neutrinos and hydro
- 35OC, fast, weak: jet-like explosion
- 35OC, fast, strong: magneto-rotational jets
- z35, slow, weak: no explosion for a very long time
- z35, fast, weak: no explosion, but sort of accretion torus

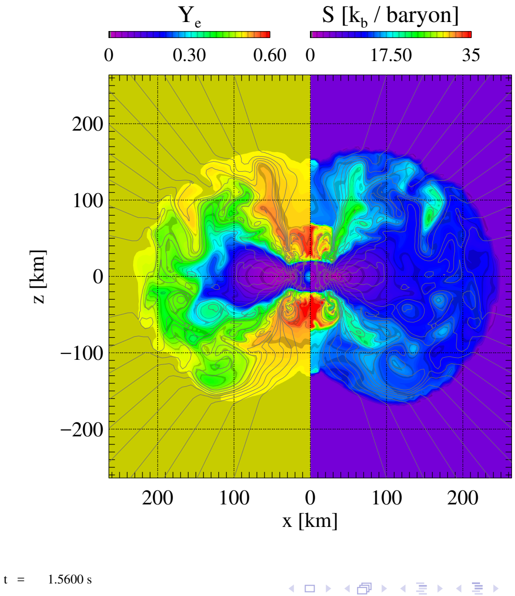

Evolutionary paths

- 35OC, moderate rotation, weak field: explodes mostly by neutrinos and hydro
- 35OC, fast, weak: jet-like explosion
- 35OC, fast, strong: magneto-rotational jets
- z35, slow, weak: no explosion for a very long time
- z35, fast, weak: no explosion, but sort of accretion torus

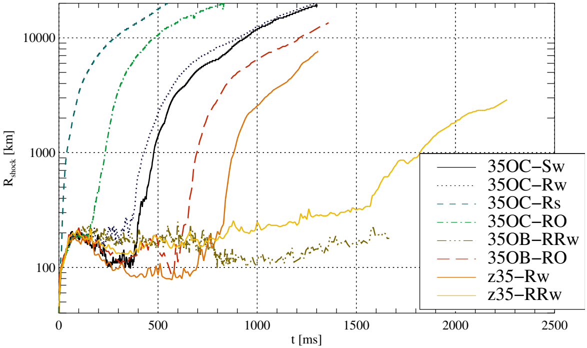

(a)

shock radii demonstrate the five different behaviours

Evolutionary paths

- 35OC, moderate rotation, weak field: explodes mostly by neutrinos and hydro
- 35OC, fast, weak: jet-like explosion
- 35OC, fast, strong: magneto-rotational jets
- z35, slow, weak: no explosion for a very long time
- z35, fast, weak: no explosion, but sort of accretion torus

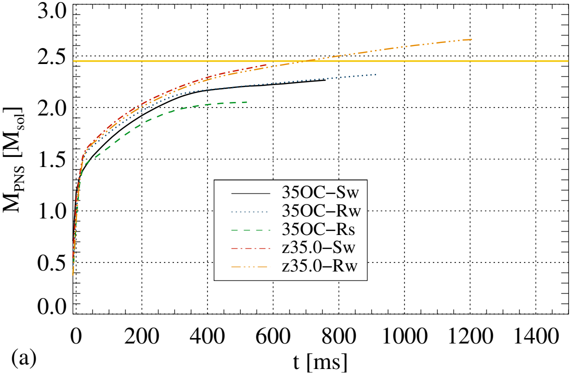

PNS masses grow even for the exploding models → BH formation conceivable

Evolutionary paths

- 35OC, moderate rotation, weak field: explodes mostly by neutrinos and hydro
- 35OC, fast, weak: jet-like explosion
- 35OC, fast, strong: magneto-rotational jets
- z35, slow, weak: no explosion for a very long time
- z35, fast, weak: no explosion, but sort of accretion torus

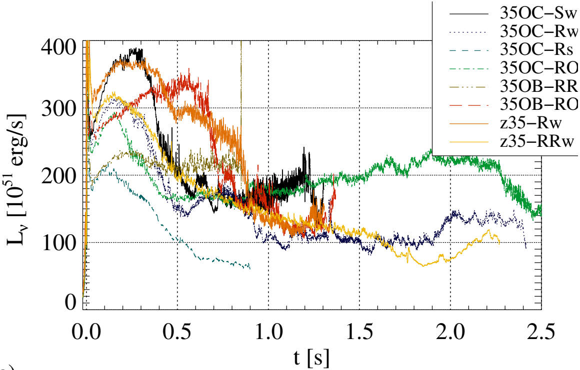

(a)

neutrino luminosities reflect the accretion history and potential explosion

Summary

- Magnetic fields may not be the most important ingredient in CCSNe and might not solve all open issues in current SN theory
- but they can have quite interesting consequences in certain (exotic?) progenitors, where they enable a wide range of physical effects.
- Currently open issues include, e.g., the development of dynamos and the field amplification by convection/SASI, the importance of the MRI, the conditions for generation of outflows and their stability.